Room temperature continuous wave operation of 1.33-μm InAs/GaAs quantum dot laser with high output power

Qin Han (韩 勤), Zhichuan Niu (牛智川), Haiqiao Ni (倪海桥), Shiyong Zhang (张石勇), Xiaohong Yang (杨晓红), Yun Du (杜 云), Cunzhu Tong (佟存柱), Huan Zhao (赵 欢), Yingqiang Xu (徐应强), Hongling Peng (彭红玲), and Ronghan Wu (吴荣汉)

State Key Laboratory on Integrated Optoelectronics, National Laboratory for Superlattices and Microstructures, Institute of Semiconductor, Chinese Academy of Sciences, Beijing 100083

Received December 13, 2005

Continuous wave operation of a semiconductor laser diode based on five stacks of InAs quantum dots (QDs) embedded within strained InGaAs quantum wells as an active region is demonstrated. At room temperature, 355-mW output power at ground state of 1.33—1.35 μm for a 20-μm ridge-waveguide laser without facet coating is achieved. By optimizing the molecular beam epitaxy (MBE) growth conditions, the QD density per layer is raised to 4×10^{10} cm^{-2}. The laser keeps lasing at ground state until the temperature reaches 65 °C.

OCIS codes: 160.6000, 140.5960.

Fabrication of semiconductor quantum dots (QDs) has received much attention for their physical interest and possible advantages in optoelectronic device applications[1−4]. QDs have been expected to drastically improve the performances of semiconductor lasers, for example, a threshold current insensitive of temperature[5,6], zero linewidth enhancement factor, a decreased transparency current density, and increased material gain which results in a very low threshold current[7,8]. GaAs-based InGaAs QD laser has been considered as one of the promising candidates for 1.3-μm long wavelength emission[9]. A great interest exists also for vertically integrating such QDs into vertical cavity surface-emitting lasers (VCSELs)[10,11]. Since the first InGaAs QD laser and first room temperature 1.3-μm QD laser were reported, InGaAs QD lasers have rapidly advanced and shown excellent performances. An extremely low threshold current densities per layer $J_{\rm th}$ = 14.7—19 A/cm^2[12−14], and ultra high characteristic temperature T_0 = 213 K[15] have been reported. However, QD lasers still have difficulty in operation at the ground state with long wavelength emission without high reflectivity coating, especially under high injection current density and high output power. Zhukov *et al.* has reported 2.7-W output power from a 200-μm-wide stripe QD laser in the range of 1.26—1.28 μm[16]. In this letter, we report high performance, 20-μm ridge-waveguide (RWG) InAs QD edge-emitting laser with 350-mW output power at the ground state with longer wavelength of 1.33—1.35 μm without facet coating. The laser is based on five stacks of InAs QDs embedded within strained InGaAs quantum wells. The QD laser with 2.9-mm cavity length operates at continuous wave (CW) operation in the ground state to a temperature of 65 °C. At room temperature, the laser has a threshold current density of 250 A/cm^2 and a differential quantum efficiency of about 45%.

The QD heterostructure was grown on (100) n-type GaAs substrate in a Veeco Mod II MBE system. The laser structure is listed in Table 1. The temperature of the growth was 600 °C, except for the QD regions. The five QD layers as active region were grown at 500 °C. The QD active region was cladded on either side by GaAs of 50 nm, and further confined in the center of an undoped 0.1-μm-thick graded index $Al_xGa_{1-x}As$ waveguide region ($x = 0 - 0.5$). The waveguide was cladded by p- and n-doped 1.5-μm-thick $Al_{0.5}Ga_{0.5}As$. Si and Be were used as the n- and p-dopants, respectively.

The QDs were formed from a 2.5 monolayer deposition of InAs on the GaAs barriers, and each layer was covered with 6-nm $In_{0.25}Ga_{0.75}As$. A 50-nm GaAs layer was used to separate the QD plane. By optimizing the molecular beam epitaxy (MBE) growth conditions, the QD density per layer is raised from 1.7×10^{10} to 4×10^{10} cm^{-2}. Room temperature photoluminescence (PL) measurement showed a ground state peak at 1.32 μm and first excited state at 1.23 μm, the well resolved energy

Table 1. Structure of QD Laser

Layer	Thickness (nm)	Doping (cm^{-3})
GaAs	50	Be, 5×10^{19}
GaAs	150	Be, 1×10^{19}
$Al_{0.5-0}GaAs$	50	Be, 1×10^{18}
$Al_{0.5}Ga_{0.5}As$	1500	Be, 1×10^{18}
$Al_{0-0.5}GaAs$	50	Undoped
GaAs	50	
$In_{0.15}Ga_{0.85}As$	6	QD Region
InAs	2.5 Mono Layer	5 Periods
⋮		
GaAs	50	
$Al_{0.5-0}GaAs$	50	Undoped
$Al_{0.5}Ga_{0.5}As$	1500	Si, 1×10^{18}
$Al_{0-0.5}GaAs$	50	Si, 1×10^{18}
GaAs	300	Si, 1×10^{18}
(100)GaAs		Si, 1×10^{18}

levels had an energy separation of 69 meV between the first state and ground states.

RWG lasers were fabricated with the 20-μm ridge formation. Following the standard photolithography process, the ridges were patterned by a self-aligned mesa etching to the p-cladding layer by wet chemical etching. The ridges were then isolated with SiO_2 by plasma enhanced chemical vapor deposition (CVD) followed by p-contact (CrAu) metallization. The wafer was lapped and polished to a thickness of 100 μm and backside AuGe/Ni/Au n-type contact was thermally evaporated. To optimize the performances of the ridge waveguide laser, the AlGaAs p-cladding layer was almost etched. The wafer was cleaved with cavity length from 1.0 to 2.9 mm. All diodes had uncoated facets.

The measured output power P_{out} from both facets versus the driving current I for the 2.9-mm-cavity-length laser in CW regime at 20 °C is presented in Fig. 1. The threshold current and the threshold current density are about 150 mA and 250 A/cm^2, respectively, and the differential slope efficiency is 45%. Experiments showed that the RWG lasers have the lowest threshold current density with stripe width from 10 to 20 μm[17]. For wider stripe, the threshold current density increases, especially under CW operation, mainly due to the heating, and the threshold current density increases for narrower stripe due to the waveguide scattering loss.

The CW lasing continues at ground state at about 1000 mA with 350-mW output power. More powers are obtained while continuously increasing the current, however the higher pump levels reveal the competition between the ground state and the first excited state transitions due to gain saturation, and the first excited state starts lasing. The laser emission spectra at different injection currents were measured with an optical spectrum analyzer (OSA), and are shown in Fig. 2. As the current increased to 1050 mA, the ground state and the first excited state lased simultaneously.

The influence of the cavity length on the state transition was investigated. Figure 3 shows room temperature CW electroluminescence (EL) spectra of QD lasers with 1.15- and 2.9-mm cavity length just below and above the threshold current. The threshold currents are 203 and 150 mA respectively. The 2.9-mm-cavity-length laser operates at 1.33 μm (solid line) corresponding to the ground state (GS), while for 1.15-mm laser the ground state saturates and the first excited state of 1.247 μm (dashed line) appears and starts lasing with current increasing to the threshold. This behavior has often been observed in QD lasers. The lasing wavelength transfer depends on the QDs gain and the cavity loss. Compared with the quantum well active region, the relative low QD density provides the low transparency current and a small maximum gain. Each QD can be filled with a certain number of carriers, and the gain depends on the QD densities ρ_{QD} and uniformity of their size distributions. Therefore the maximal achievable gain is limited and can be insufficient for lasing at some losses. So reducing the cavity loss can decrease the threshold gain, and increasing the number of dot layers can lower the

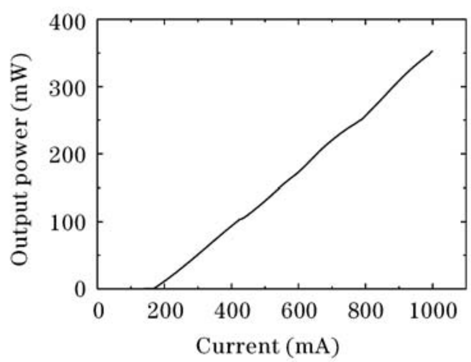

Fig. 1. Output power (from both facets) versus current for a 2.9-mm-cavity-length QD laser without facet coating at room temperature (293 K).

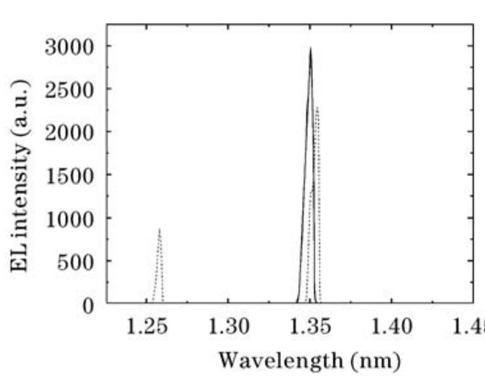

Fig. 2. EL spectra of the 2.9-mm-cavity-length QD laser measured at 1000 mA (solid line) and 1050 mA (dashed line) at room temperature.

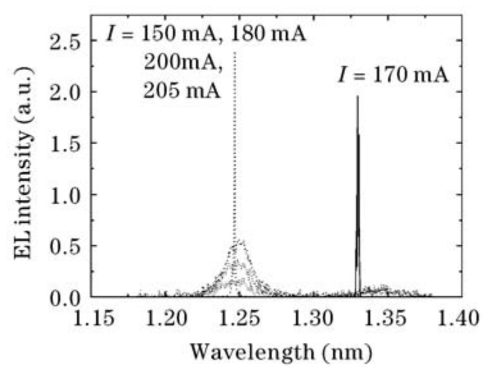

Fig. 3. EL spectra of 1.15-mm (dashed line) and 2.9-mm (solid line) cavity length QD lasers below and above threshold current of 203 and 150 mA, respectively, at room temperature.

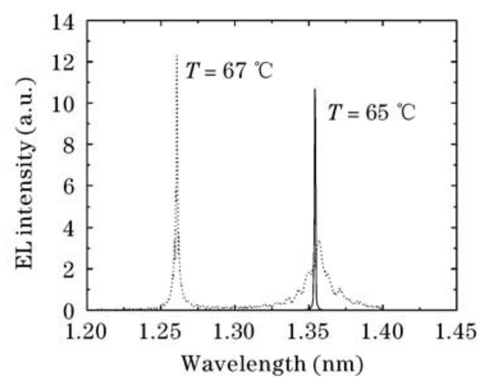

Fig. 4. EL spectra of a 2.9-mm-cavity-length QD laser measured at 65 °C (solid line) and 67 °C (dashed line), indicating a wavelength switching between ground state and first excited state.

threshold gain per dot layer, both promote the ground state lasing before the gain saturated. By fitting the relationship between the differential slope efficiency and the cavity length, the internal loss of 1.59 cm^{-1} and the internal quantum efficiency of 59% were derived.

The temperature dependence of lasing wavelength transfer was also investigated. Figure 4 shows the spectral characteristic of the 2.9-mm-cavity-length laser at 65 and 67 °C under CW operation. At 65 °C the lasers still keep lasing at ground state (solid line) and then transfer to the first excited state with temperature increasing up to 67 °C (dashed line). Temperature dependence of the lasing wavelength shift under 65 °C of 0.5 nm/°C was measured under pulsed operation.

In summary, we have demonstrated high power CW operation of a QD laser with five stacks of an InAs QD layer embedded within InGaAs quantum wells. At room temperature, 350-mW output power is achieved at 1.33—1.35 μm from both facets without facet coating for a 2.9-mm-length-cavity QD laser. The internal quantum efficiency is 59%, and with the total QD density of 2×10^{11} cm^{-2} for the active region the laser keeps lasing at ground state until the temperature reaches 65 °C.

This work was supported by the Major State Key Basic Research Program (No. TG2000036603), the National "863" Program of China (No. 2002AA312080), and the National Natural Science Foundation of China (No. 60137020). Q. Han's e-mail address is hanqin @red.semi.ac.cn.

References

1. N. Kirstaedter, N. N. Ledentsov, M. Grundmann, D. Bimberg, V. M. Ustinov, S. S. Ruvimov, M. V. Macimov, P. S. Kop'ev, Zh. I. Alferov, U. Richter, P. Werner, U. Gosele, and J. Heydenreich, Electron. Lett. **30,** 1416 (1994).
2. H. Shoji, K. Mukai, N. Ohtsuka, M. Sugawara, T. Uchida, and H. Ischikawa, IEEE Photon. Technol. Lett. **7,** 1385 (1995).
3. K. Kamath, P. Bhattacharya, T. Sosnowski, T. Norris, and J. Phillips, Electron. Lett. **32,** 1374 (1996).
4. D. L. Huffaker, G. Park, Z. Zou, O. B. Shchekin, and D. G. Deppe, Appl. Phys. Lett. **73,** 2564 (1998).
5. O. B. Schekin and D. G. Deppe, Appl. Phys. Lett. **80,** 3277 (2002).
6. Y. Arakawa and H. Sakaki, Appl. Phys. Lett. **40,** 939 (1982).
7. Y. Arakawa and A. Yariv, IEEE J. Quantum Electron. **22,** 1887 (1986).
8. M. Asada, Y. Miyamoto, and Y. Suematsu, IEEE J. Quantum Electron. **22,** 1915 (1986).
9. R. Fehse, I. Marko, and A. R. Adams, IEE Proc.—Circuits Device Syst. **150,** 521 (2003).
10. D. L. Huffaker, H. Deng, and D. G. Deppe, IEEE Photon. Technol. Lett. **10,** 185 (1998).
11. N. Ledentsov, D. Bimberg, V. M. Ustinov, Zh. I. Alferov, and J. A. Lott, Physica E **13,** 871 (2001).
12. R. Krebs, F. Klopf, J. P. Reithmaier, and A. Forchel, Jpn. J. Appl. Phys. **41,** 1158 (2002).
13. O. B. Shchekin, G. Park, D. L. Huffaker, Q. Mo, and D. G. Deppe, IEEE Photon. Technol. Lett. **12,** 1120 (2000).
14. Y. Qiu, P. Gogna, S. Forouhar, A. Stinz, and L. F. Lester, Appl. Phys. Lett. **79,** 3570 (2001).
15. O. B. Shchekin, J. Ahn, and D. G. Deppe, Electron. Lett. **38,** 712 (2002).
16. A. E. Zhukov, A. R. Kovsh, V. M. Ustinov, Yu. M. Shernyakov, S. S. Ruvimov, N. A. Maleev, E. Yu. Kondrat'eva, D. A. Livshits, M. V. Maximov, B. V. Volovik, D. A. Bedarev, Yu. G. Musikhin, N. N. Ledentsov, P. S. Kop'ev, Zh. I. Alferov, and D. Bimberg, IEEE Photon. Technol. Lett. **11,** 1345 (1999).
17. G. Park, O. B. Shchekin, S. Csutak, D. L. Huffaker, and D. G. Deppe, Appl. Phys. Lett. **75,** 3267 (1999).